

Observations of the Blazar 3C 66A with the MAGIC Telescopes in Stereoscopic Mode

J. Aleksić^a, L. A. Antonelli^b, P. Antoranz^c, M. Backes^d, J. A. Barrio^e, D. Bastieri^f,
J. Becerra González^{g,h}, W. Bednarekⁱ, A. Berdyugin^j, K. Berger^g, E. Bernardini^k,
A. Biland^l, O. Blanch^a, R. K. Bock^m, A. Boller^l, G. Bonnoli^b, P. Bordasⁿ, D. Borla
Tridon^m, V. Bosch-Ramonⁿ, D. Bose^e, I. Braun^l, T. Bretz^o, M. Camara^e, A. Cañellasⁿ,
E. Carmona^m, A. Carosi^b, P. Colin^m, E. Colombo^g, J. L. Contreras^e, J. Cortina^a,
L. Cossio^p, S. Covino^b, F. Dazzi^{p,*}, A. De Angelis^p, E. De Cea del Pozo^q, B. De Lotto^p,
M. De Maria^p, F. De Sabata^p, C. Delgado Mendez^{g,**}, A. Diago Ortega^{g,h}, M. Doert^d,
A. Domínguez^r, D. Dominis Prester^s, D. Dorner^l, M. Doro^f, D. Elsaesser^o, M. Errando^a,
D. Ferenc^s, M. V. Fonseca^e, L. Font^t, R. J. García López^{g,h}, M. Garzarczyk^g, G. Giavitto^a,
N. Godinović^s, D. Hadasch^q, A. Herrero^{g,h}, D. Hildebrand^l, D. Höhne-Mönch^o, J. Hose^m,
D. Hrupec^s, T. Jogler^m, S. Klepser^a, T. Krähenbühl^l, D. Kranich^l, J. Krause^m, A. La
Barbera^b, E. Leonardo^c, E. Lindfors^j, S. Lombardi^f, F. Longo^p, M. López^e, E. Lorenz^{l,m},
P. Majumdar^k, M. Makariev^u, G. Maneva^u, N. Mankuzhiyil^p, K. Mannheim^o, L. Maraschi^b,
M. Mariotti^f, M. Martínez^a, D. Mazin^a, M. Meucci^c, J. M. Miranda^c, R. Mirzoyan^m,
H. Miyamoto^m, J. Moldónⁿ, A. Moralejo^a, D. Nieto^e, K. Nilsson^{j,***}, R. Orito^m, I. Oya^e,
R. Paoletti^c, J. M. Paredesⁿ, S. Partini^c, M. Pasanen^j, F. Paus^l, R. G. Pegna^c,
M. A. Perez-Torres^r, M. Persic^{p,v}, L. Peruzzo^f, J. Pochon^g, F. Prada^r, P. G. Prada
Moroni^c, E. Prandini^f, N. Puchades^a, I. Puljak^s, I. Reichardt^a, R. Reinthal^j, W. Rhode^d,
M. Ribónⁿ, J. Rico^{w,a}, S. Rügamer^o, A. Saggion^f, K. Saito^m, T. Y. Saito^m, M. Salvati^b,
M. Sánchez-Conde^{g,h}, K. Satalecka^k, V. Scalzotto^f, V. Scapin^p, C. Schultz^f, T. Schweizer^m,
M. Shayduk^m, S. N. Shore^x, A. Sierpowska-Bartosikⁱ, A. Sillanpää^j, J. Sitarek^{m,i},
D. Sobczynskaⁱ, F. Spanier^o, S. Spiro^b, A. Stamerra^c, B. Steinke^m, J. Storz^o, N. Strah^d,
J. C. Struebig^o, T. Suric^s, L. Takalo^j, F. Tavecchio^b, P. Temnikov^u, T. Terzić^s, D. Tescaro^a,
M. Teshima^m, M. Thom^d, D. F. Torres^{w,q}, H. Vankov^u, R. M. Wagner^m, Q. Weitzel^l,
V. Zabalzaⁿ, F. Zandanel^r, R. Zanin^a,
ksaito@mppmu.mpg.de, klepser@ifae.es

ABSTRACT

We report new observations of the intermediate-frequency peaked BL Lacertae object 3C 66A with the MAGIC telescopes. The data sample we use was taken in 2009 December and 2010 January, and comprises 2.3 hours of good quality data in stereoscopic mode. In this period, we find a significant signal from the direction of the blazar 3C 66A. The new MAGIC stereoscopic system is shown to play an essential role for the separation between 3C 66A and the nearby radio galaxy 3C 66B, which is at a distance of only 6'. The derived integral flux above 100 GeV is 8.3% of Crab Nebula flux and the energy spectrum is reproduced by a power law of photon index $3.64 \pm 0.39_{\text{stat}} \pm 0.25_{\text{sys}}$. Within errors, this is compatible with the one derived by VERITAS in 2009. From the spectra corrected for absorption by the extragalactic background light, we only find small differences between the four models that we applied, and constrain the redshift of the blazar to $z < 0.68$.

Subject headings: BL Lacertae objects: individual (3C 66A) — galaxies: active — gamma rays: galaxies

1. Introduction

Blazars are the majority of extragalactic sources of very high energy (VHE, $E > 100$ GeV) gamma-rays. They are a subset of active galactic nuclei (AGN), and consist of BL Lacertae (BL Lac) objects and flat-spectrum radio-loud quasars (FS-RQs). The general framework to explain the

gamma-ray emission is that they are produced by charged particles which are accelerated in a relativistic jet. These jets are powered by gas accretion into a central supermassive black hole and are perpendicular to the accretion disc. When the jet is directed to us, the energy and flux of gamma-rays are boosted by the relativistic beaming effect (e.g. Blandford & Rees 1978; Urry & Padovani 1995).

Generally, the spectral energy distribution (SED) of AGNs can be described by two broad bumps. The lower energetic bump, at frequencies from radio to X-rays, is attributed to synchrotron emission from nonthermal relativistic electrons in the jet. The other bump, covering the X-ray to gamma-ray bands, could either be due to inverse Compton scattering of seed photons by the electrons (leptonic model, e.g. Maraschi et al. 1992; Dermer & Schlickeiser 1993; Bloom & Marscher 1996; Krawczynski 2004) or due to hadronic interactions (see e.g. Mannheim 1993; Mücke & Protheroe 2001; Mücke et al. 2003).

3C 66A was classified as a BL Lac object by Maccagni et al. (1987), based on its significant optical and X-ray variability. The synchrotron peak of this source is located between 10^{15} and 10^{16} Hz (Perri et al. 2003), therefore 3C 66A can also be classified as an intermediate-frequency peaked BL Lac object (IBL). The redshift of 3C 66A was determined to be $z = 0.444$ by independent authors (Miller et al. 1978; Lanzetta et al. 1993). However, their measurements are based on the detection of one single line. Another observation of 3C 66A at a different spectral range was reported by Finke et al. (2008), but no spectral feature was found, and a lower limit of the redshift was derived to be 0.096. For the marginally resolved host galaxy (Wurtz et al. 1996), a redshift of 0.321 was found. Recently, through the investigation of the Large Area Telescope (LAT), on board the Fermi Gamma-ray Space Telescope (Fermi) satellite and VHE gamma-ray observations, upper limits for the redshift of 3C 66A were derived; $z = 0.44$ (Prandini et al. 2010, 2σ confidence level) and $z = 0.58$ (Yang & Wang 2010).

Several gamma-ray observations of 3C 66A were performed since the 1990s. With the EGRET satellite, a GeV gamma-ray emission (3EG J0222+4253) was associated with 3C 66A (Hartman et al. 1999). However, due to the large

^aIFAE, Edifici Cn., Campus UAB, E-08193 Bellaterra, Spain

^bINAF National Institute for Astrophysics, I-00136 Rome, Italy

^cUniversità di Siena, and INFN Pisa, I-53100 Siena, Italy

^dTechnische Universität Dortmund, D-44221 Dortmund, Germany

^eUniversidad Complutense, E-28040 Madrid, Spain

^fUniversità di Padova and INFN, I-35131 Padova, Italy

^gInst. de Astrofísica de Canarias, E-38200 La Laguna, Tenerife, Spain

^hDepto. de Astrofísica, Universidad de La Laguna, E-38206 La Laguna, Spain

ⁱUniversity of Łódź, PL-90236 Lodz, Poland

^jTuorla Observatory, University of Turku, FI-21500 Piikkiö, Finland

^kDeutsches Elektronen-Synchrotron (DESY), D-15738 Zeuthen, Germany

^lETH Zurich, CH-8093 Switzerland

^mMax-Planck-Institut für Physik, D-80805 München, Germany

ⁿUniversitat de Barcelona (ICC/IEEC), E-08028 Barcelona, Spain

^oUniversität Würzburg, D-97074 Würzburg, Germany

^pUniversità di Udine, and INFN Trieste, I-33100 Udine, Italy

^qInstitut de Ciències de l'Espai (IEEC-CSIC), E-08193 Bellaterra, Spain

^rInst. de Astrofísica de Andalucía (CSIC), E-18080 Granada, Spain

^sCroatian MAGIC Consortium, Institute R. Boskovic, University of Rijeka and University of Split, HR-10000 Zagreb, Croatia

^tUniversitat Autònoma de Barcelona, E-08193 Bellaterra, Spain

^uInst. for Nucl. Research and Nucl. Energy, BG-1784 Sofia, Bulgaria

^vINAF/Osservatorio Astronomico and INFN, I-34143 Trieste, Italy

^wICREA, E-08010 Barcelona, Spain

^xUniversità di Pisa, and INFN Pisa, I-56126 Pisa, Italy

* supported by INFN Padova

** now at: Centro de Investigaciones Energéticas, Medioambientales y Tecnológicas

*** now at: Finnish Centre for Astronomy with ESO (FINCA), Turku, Finland

EGRET point spread function, an influence by the nearby pulsar PSR J0218+4232 could not be excluded (Kuiper et al. 2000). The Crimean Astrophysical Observatory claimed detections of 3C 66A above 900 GeV with an integral flux of $(3 \pm 1) \times 10^{-11} \text{ cm}^{-2} \text{ s}^{-1}$ (Stepanyan et al. 2002). Later observations by HEGRA and Whipple reported upper limits of $F(> 630 \text{ GeV}) < 1.42 \times 10^{-11} \text{ cm}^{-2} \text{ s}^{-1}$ (Aharonian et al. 2000) and $F(> 350 \text{ GeV}) < 0.59 \times 10^{-11} \text{ cm}^{-2} \text{ s}^{-1}$ (Horan et al. 2004), respectively. Additionally, the STACEE observation found a hint of signals at a 2.2 significance level and derived upper limits of $< 1.0 \times 10^{-11} \text{ cm}^{-2} \text{ s}^{-1}$ and $< 1.8 \times 10^{-11} \text{ cm}^{-2} \text{ s}^{-1}$ for thresholds of 147 GeV and 200 GeV, respectively (Bramel et al. 2005).

Recent VERITAS observations of 3C 66A taken from 2007 September to 2008 January and from 2008 September to 2008 November, for a total of 32.8 hours, resulted in a detection in VHE gamma rays (Acciari et al. 2009). The energy spectrum was derived with a photon index of $\Gamma = 4.1 \pm 0.4_{\text{stat}} \pm 0.6_{\text{sys}}$. The integral flux of the VERITAS observations above 200 GeV is $(1.3 \pm 0.1) \times 10^{-11} \text{ cm}^{-2} \text{ s}^{-1}$ (6 % of the Crab Nebula flux).

3C 66A has been monitored by Fermi/LAT since 2008 August, covering the latter part of the VERITAS observation. According to Abdo et al. (2009), which reported the first 5.5 months of Fermi/LAT observations of 3C 66A, the blazar showed a significant flux variability (a factor of 5-6 between the highest and lowest fluxes). The derived energy spectrum with the photon index of $\Gamma = 1.98$ above 1 GeV, in combination with the VERITAS spectrum, indicates that the spectrum must soften above 100 GeV.

MAGIC observed the sky region around 3C 66A from 2007 August to December, obtaining a total exposure time after data quality cuts of 45.3 hours (Aliu et al. 2009b). These data revealed a significant VHE gamma-ray signal centered at $2^{\text{h}}23^{\text{m}}12^{\text{s}}$, $43^{\circ}0'7''$. This excess (named MAGIC J0223+430) coincides within uncertainties with the position of a nearby, Fanaroff-Riley-I (FRI) type galaxy 3C 66B ($z = 0.0215$, Stull et al. 1975). Still, judging from the skyplot alone, the probability of the emission to originate from 3C 66A is 14.6 %. The energy spectrum of MAGIC J0223+430 was reproduced by a single power-law with the index of

$\Gamma = 3.1 \pm 0.3$. The integral flux above 150 GeV corresponded to $(7.3 \pm 1.5) \times 10^{-12} \text{ cm}^{-2} \text{ s}^{-1}$ (2.2 % of the Crab Nebula flux). According to Tavecchio & Ghisellini (2008), the radio galaxy is also a plausible source of VHE gamma-ray radiation. Also, the recent MAGIC detection of IC 310 (Mariotti et al. 2010), a radio galaxy at a very similar redshift ($z = 0.0189$) indicates that 3C 66B might be feasible to explain all or part of the MAGIC detection from 2007.

2. Observations

From mid-August 2009, 3C 66A went into an optical high state which was reported by the Tuorla blazar monitoring program¹. This outburst triggered new MAGIC observations. The optical flux in the R-band reached a maximum level of $\sim 12 \text{ mJy}$ in January 2010, while the baseline flux in the historical data of the source is $\sim 6 \text{ mJy}$.

The observations were carried out with the MAGIC telescopes located on the Canary Island of La Palma (28.8° N , 17.8° W , 2220 m a.s.l.). The two 17 m diameter telescopes use the atmospheric Cherenkov imaging technique and allow for measurements at a threshold as low as 50 GeV in normal trigger mode.

We observed the blazar 3C 66A in several time slots between September 2009 and January 2010. However, the sky imaging CCD cameras that are used to cross-check the telescope pointing ("starguider cameras") only became fully applicable to stereo observations in early December. To allow for a high-confidence directional statement on the arcminute scale, we therefore only used data taken after these upgrades, which were 5.6 hours in total. Furthermore, we had to discard data with low event rates, affected by the exceptionally bad weather conditions in that winter. Finally, we had 2.3 hours of good quality data left after all quality cuts. They were taken on 6 days between 2009 December 5 and 2010 January 18, partly under low intensity moon light conditions.

The data were taken using the false source tracking (wobble) method (Fomin et al. 1994), in which the pointing direction alternates every 20 minutes between two positions, offset by $\pm 0.4^{\circ}$ in

¹<http://users.utu.fi/kani/1m/index.html>

RA from the source. These wobble positions were chosen with respect to 3C 66A, but the small distance to 3C 66B (0.01°) allows equal judgment for both sources. The data were taken at zenith angles between 13° and 35° .

3. Data Analysis

For the analysis, only stereoscopic events triggered by both MAGIC telescopes were used. They were analysed in the MARS analysis framework (Moralejo et al. 2009), taking advantage both of the advanced single-telescope algorithms (e.g. Aliu et al. 2009a) and newly developed stereoscopic analysis routines. These routines are at present still subject to some minor improvements and will be discussed in more detail in a separate paper still in preparation, but are shortly outlined in the following.

Combining monoscopic and stereoscopic strategies, the direction of gamma rays is calculated for each telescope separately, using the random forest technique (Albert et al. 2008b), and later combined with the projected crossing point of the image axes, with a weight depending on the angle between the two shower images. Requiring a certain level of agreement between the different estimates furthermore improves the resolution, and also helps to reject hadron showers, whose directional information tends to be fuzzier than the one of photon showers.

Similarly, an energy estimator is determined from look-up tables for each telescope separately. The tables are generated through Monte Carlo simulations (MC), and characterize the energy as a function of reconstructed impact parameters and the total number of photons of a shower. In the end, the two estimates are averaged to get a common estimated energy.

The skymap generation, which is particularly important for the analysis of data from the 3C 66A/B region, follows a two-step algorithm. The first step is to generate an exposure model for the field of view in camera coordinates, for the quality cuts that were applied in the analysis. This is done by joining the distributions of photon-like events from the two wobble positions, taking advantage of the fact that the source, in relative camera coordinates, is on opposite sides for both wobble sets. The exposure model does

not only depend on the camera coordinates, but also on the zenith and azimuth angles because the shape of the sensitive area depends on the relative position of the two telescopes with respect to the pointing direction.

The second step is the calculation of an expected background event distribution in celestial coordinates, and its comparison to the actual event distribution. Before that comparison, a smearing with a Gaussian kernel is applied. The significances are calculated following equation (17) of Li & Ma (1983), taking into account the higher precision of the background estimation implied by the above modelling.

The performance of the analysis software was optimized and checked with contemporaneous Crab Nebula data and MC. The Crab Nebula spectrum could be analysed down to about 50 GeV, fully covering the range of the spectrum presented in the next paragraph. The achieved angular resolution, defined as the σ of a two-dimensional Gaussian function, is around 0.1° at 100 GeV and approaching 0.065° at higher energies. This σ defines the radius in which 39% of all photons of a point source are contained. The systematic uncertainty on the direction reconstruction is a product of the telescope pointing uncertainty and possible biases that occur in the reconstruction algorithms. The latter can be caused by irregularities in the shower images, such as missing camera pixels, inhomogeneous noise from stars in the field of view, or imperfections in the data acquisition electronics. Both the total pointing deviation and the telescope pointing precision of MAGIC were always monitored over the years (Bretz et al. 2009; Aleksić et al. 2010), and along with studies of contemporary stereo data of known direction lead to an estimate of the maximal systematic stereoscopic pointing uncertainty of 0.025° .

We also used the publicly accessible Fermi/LAT data from the HEASARC web site² to investigate the status of the source in the GeV energy range during the MAGIC observation period. The Fermi data were analyzed using the public software package LAT Science Tools v9.15.2, including the Instrument Response File P6_V3_DIFFUSE, and galactic, extragalactic and instrumental background models.

²<http://fermi.gsfc.nasa.gov/>

4. Results

Figure 1 shows a skymap of the observed region above 100 GeV. The significance of the excess at the location of 3C 66A is 6.4σ . We cross-checked the detection also by investigating the distribution of squared angular distances (θ^2) between photon directions and the assumed source position. The expected background is extracted from corresponding θ^2 -plots done with respect to other sky positions at similar distance from the pointing direction. Comparing the data with this expectation we find a significance of 5.2σ (see Figure 2). The difference in significance can be attributed to the different integration procedure of signal and background in the skymap, which generally leads to a slightly better background estimation and therefore a higher significance.

We also analysed the data taken with and without moon light separately to find possible effects from the higher thresholds of individual camera pixels. However, we could not find a clear tendency beyond the statistical errors and thus decided to use all the data for the analysis.

Unlike in the 2007 observations of this sky region, the emission peak this time is clearly on top of 3C 66A. The fitted center of gravity of the excess (small black square in Figure 1) is at a distance of $0.010^\circ \pm 0.023^\circ$ (stat.) $\pm 0.025^\circ$ (sys.) from 3C 66A, and $0.108^\circ \pm 0.023^\circ$ (stat.) $\pm 0.025^\circ$ (sys.) from 3C 66B. While being compatible with the former, the statistical rejection power for the emission to emerge from the radio galaxy 3C 66B corresponds to 4.6 standard deviations. Even considering the unlikely case of a systematic offset exactly towards the blazar, the rejection significance of 3C 66B is at least 3.6σ . These numbers were confirmed by a second analysis with independent data quality selection and cut optimization procedures. The same result is found even when the photon direction is taken only from the projected crossing point of the two shower axes. We therefore conclude that the signal we see this time emerges from the blazar 3C 66A.

It shall be mentioned that this result is a clear merit of the angular resolution and background rejection of the new stereoscopic system. In fact, if we compare the above stereo directional reconstruction algorithm to the MAGIC-I algorithm alone, we find basically the same result, but the

statistical error of the fitted source position increases roughly by a factor of two. Consequently, the rejection significance of 3C 66B would be less than 2 standard deviations, and the total detection significance would be below 5 standard deviations.

The energy spectrum of 3C 66A was derived using four different unfolding algorithms (Albert et al. 2007). We found that the data are well compatible with a power law of the form

$$\frac{dF}{dE} = K_{200} \left(\frac{E}{200 \text{ GeV}} \right)^{-\Gamma} \quad (1)$$

with a photon index $\Gamma = 3.64 \pm 0.39_{\text{stat}} \pm 0.25_{\text{sys}}$ and a flux constant at 200 GeV of $K_{200} = 9.6 \pm 2.5_{\text{stat}} \pm 3.4_{\text{sys}} \times 10^{-11} \text{ cm}^{-2} \text{ s}^{-1} \text{ TeV}^{-1}$. The integral flux above 100 GeV corresponds to $(4.5 \pm 1.1) \times 10^{-11} \text{ cm}^{-2} \text{ s}^{-1}$ (8.3% Crab Nebula flux). Here, the parameters and statistical errors are taken from the forward unfolding method, while the systematic errors reflect the variations among the different unfolding algorithms, plus several standard uncertainties discussed in Albert et al. (2008a). The systematic flux uncertainties add up to 36% in total. Figure 3 displays the spectrum we derived.

We also analysed the Fermi data from the same time period, and found a moderate day-to-day variability, and a photon index compatible with the one found in Abdo et al. (2009), indicating no significant change in the overall spectral shape.

5. Discussions and Conclusions

MAGIC observed the 3C 66A/B region in December 2009 and January 2010, during an optical active state of 3C 66A and detected a clear VHE gamma-ray signal. The excess coincides with the position of 3C 66A, and we rule out the emission to come from 3C 66B at a confidence level of 3.6σ . This detection does not contradict the earlier MAGIC detection, though, which favored 3C 66B as the VHE source. On the one hand, because the observation time of 2.3 hours would be too short to detect the VHE emission of 3C 66B, if on a similar flux level as in 2007, and on the other hand, because its flux may be even lower than before. In fact, 3C 66A might have to be in a low flux state in order not to outshine the comparably weak emission from 3C 66B at this close distance of about 1σ of the PSF of the MAGIC telescopes.

The obtained energy spectrum is softer than in the previous MAGIC detection ($\Gamma = 3.10 \pm 0.31_{\text{stat}} \pm 0.2_{\text{sys}}$), and compatible with the VERITAS spectrum of 3C 66A. Compared to VERITAS, the MAGIC measurement has a lower threshold and the spectrum is extending to well below 100 GeV. The flux level of 8.3% Crab Nebula flux is similar to the one reported by VERITAS (6%), and significantly higher than in the previous MAGIC observation (2.2%).

Due to the shortness of the observation, we cannot discuss flux variability with these data. However, comparing the flux to the one from our previous observation of the 3C 66A/B region confirms the VERITAS report of 3C 66A being a variable source in general.

The VHE photons can be absorbed by pair production with the low energy (UV to infrared) photons of extragalactic background light (EBL) (Stecker et al. 1992; Hauser & Dwek 2001). The absorption depends on the energy and the redshift. To derive an EBL corrected spectrum, we tested several state of the art EBL models, Franceschini et al. (2008), the fiducial model in Gilmore et al. (2009), Kneiske & Dole (2010) and Domínguez et al. (2010). The EBL corrections were applied in the spectrum unfolding procedure, using the covariance matrix to correctly calculate the errors. The spread of the EBL corrected, mean flux values, obtained by the four models assuming the redshift of $z = 0.444$, is shown in Figure 3. The EBL corrected indices of our data using different modelings of the EBL are listed in Table 1. The differences between the obtained spectra are very small, although the one corrected after Kneiske & Dole (2010) is slightly harder than the others. This reflects the fact that also the predicted EBL shapes and densities are very similar in the first three models, but the overall density in Kneiske & Dole (2010) is somewhat higher.

Since the obtained index is still within the range of possible VHE emission models, and given the Fermi index of 1.98, the assumed redshift of $z = 0.444$ does not contradict our observations. In fact, we investigated the plausibility of the redshift, assuming that the intrinsic spectrum is not expected to be exponentially rising, and thus have a *pile-up*, at highest energies (see Mazin & Goebel 2007; Mazin & Raue 2007). Using the Franceschini et al. (2008) model and the likelihood ratio

test between the "power law" and "power law + pile-up" hypotheses, we derive an upper limit on the redshift of $z < 0.68$.

The results derived in this paper demonstrate the advantages of the MAGIC stereoscopic system. Further MAGIC and other gamma-ray observations of this region can provide interesting information about the IBL type BL Lac object 3C 66A, and, during low flux periods of that, also the FRI type galaxy 3C 66B.

6. Acknowledgments

We would like to thank the Instituto de Astrofísica de Canarias for the excellent working conditions at the Observatorio del Roque de los Muchachos in La Palma. The support of the German BMBF and MPG, the Italian INFN, the Swiss National Fund SNF, and the Spanish MICINN is gratefully acknowledged. This work was also supported by the Marie Curie program, by the CPAN CSD2007-00042 and MultiDark CSD2009-00064 projects of the Spanish Consolider-Ingenio 2010 programme, by grant DO02-353 of the Bulgarian NSF, by grant 127740 of the Academy of Finland, by the YIP of the Helmholtz Gemeinschaft, by the DFG Cluster of Excellence "Origin and Structure of the Universe", and by the Polish MNiSzW Grant N N203 390834. The Fermi data were obtained from the High Energy Astrophysics Science Archive Research Center (HEASARC), provided by NASA's Goddard Space Flight Center.

REFERENCES

- Abdo, A. A., et al. 2009, *ApJ*, 707, 1310
- Acciari, V. A., et al. 2009, *ApJ*, 693, L104
- Aharonian, F., et al. 2000, *A&A*, 353, 847
- Albert, J. et al. 2007, *Nucl. Instr. Meth. A*, 583, 494
- Albert, J. et al. 2008a, *ApJ*, 674, 1037
- Albert, J. et al. 2008b, *Nucl. Instr. Meth. A*, 588, 424
- Aleksić, J. et al. 2010, submitted to *ApJ*, preprint arXiv:1004.1093
- Aliu, E. et al. 2009a, *Astropart. Phys.*, 30, 293
- Aliu, E., et al. 2009b, *ApJ*, 692, L29
- Blandford, R. D., & Rees, M. J., 1978, in *Pittsburgh Conf. BL Lac Objects*, ed. A. M. Wolfe (Univ. Pittsburgh, PA), 328
- Bloom, S. D., & Marscher, A. P. 1996, *ApJ*, 461, 657
- Bramel, D. A., et al. 2005, *ApJ*, 629, 108
- Bretz, T., Dorner, D., Wagner, R. M., Sawallisch, P. 2009, *Astropart. Phys.*, 31, 92
- Dermer, C. D., & Schlickeiser, R. 1993, *ApJ*, 416, 458
- Domínguez, A., et al. 2010, *MNRAS*, in press (arXiv:1007.1459)
- Finke, J. D., Shields, J. C., Böttcher, M., & Basu, S. 2008, *A&A*, 477, 513
- Fomin, V. P., Stepanian, A. A., Lamb, R. C., Lewis, D. A., Punch, M., Weekes, T. C. 1994, *Astropart. Phys.*, 2, 137
- Franceschini, A., Rodighiero, G., & Vaccari, M. 2008, *A&A*, 487, 837
- Gilmore, R. C., Madau, P., Primack, J. R., Somerville, R. S., & Haardt, F. 2009, *MNRAS*, 399, 1694
- Hauser, M. G., & Dwek, E. 2001, *ARA&A*, 39, 249
- Hartman, R. C., et al. 1999, *ApJS*, 123, 79
- Horan, D., et al. 2004, *ApJ*, 603, 51
- Kneiske, T. M., & Dole, H. 2010, *A&A*, 515, A19
- Krawczynski, H. 2004, *New A Rev.*, 48, 367
- Kuiper, L., Hermsen, W., Verbunt, F., Thompson, D. J., Stairs, I. H., Lyne, A. J., Strickman, M. S., & Cusumano, G. 2000, *A&A*, 359, 5
- Lanzetta, K. M., Turnshek, D. A., & Sandoval, J. 1993, *ApJS*, 84, 109
- Li, T.P., Ma, Y.Q. 1983, *ApJ*, 272, 317
- Maccagni, D., Garillini, B., Schild, R., & Tarengi, M. 1987, *A&A*, 178, 21
- Mannheim, K. 1993, *A&A*, 269, 67
- Maraschi, L., Ghisellini, G., & Celotti, A. 1992, *ApJ*, 397, 5
- Mariotti, M. et al. 2010, *The Astronomer's Telegram*, 2510
- Mazin, D., & Goebel, F. 2007, *ApJ*, 655, L13
- Mazin, D., & Raue, M. 2007, *A&A*, 471, 439
- Miller, J. S., French, H. B., & Hawley, S. A. 1978, in *Pittsburgh Conf. BL Lac Objects*, ed. A. M. Wolfe (Univ. Pittsburgh, PA), 176
- Moralejo, A. et al. 2009, in *Proc. 31st ICRC (Łódź)*, preprint arXiv:0907.0943
- Mücke, A., & Protheroe, R. J. 2001, *Astropart. Phys.*, 15, 121
- Mücke, A., Protheroe, R. J., Engel, R., Rachen, J. P., & Stanev, T. 2003, *Astropart. Phys.*, 18, 593
- Perri, M., et al. 2003, *A&A*, 407, 453
- Prandini, E., Bonoli, G., Maraschi, L., Mariotti, M., & Tavecchio, F. 2010, *MNRAS*, 405, L76
- Stecker, F. W., de Jager, O. C., & Salamon, M. H. 1992, *ApJ*, 390, L49
- Stepanyan, A. A., Neshpor, Y. I., Andreeva, N. A., Kalekin, O. P., Zhogolev, N. A., Fomin, V. P., & Shitov, V. G. 2002, *Astron. Rep.*, 46, 634

- Stull, M. A., et al. 1975, AJ, 80, 559
- Tavecchio, F., & Ghisellini, G. 2008, MNRAS, 394, L131
- Tikhonov, A.N., & Arsenin, V.J., Methods for the solution of ill-posed problems (Nauka, 1979)
- Urry, M. & Padovani, P. 1995, PASP, 107, 803
- Wurtz, R., Stocke, J. T., & Yee, H. K. C. 1996, ApJS, 103, 109
- Yang, J., & Wang, J. 2010, PASJ, in press (arXiv:1006.4401)

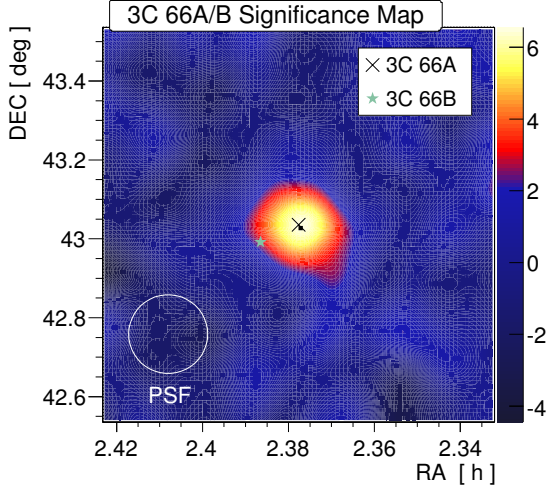


Fig. 1.— MAGIC significance skymap of the region around 3C 66A/B for events with energies above 100 GeV.

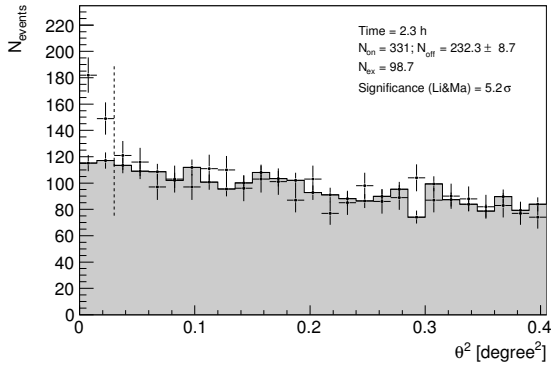


Fig. 2.— Distribution of squared angular distances between photon directions and the position of 3C 66A (θ^2) for events with energies above 100 GeV. The OFF data are taken from three positions that are symmetrical with respect to the telescope pointing directions.

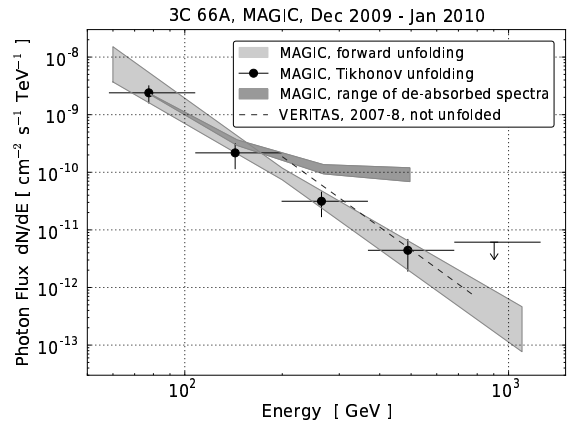


Fig. 3.— Differential energy spectrum of 3C 66A in the period of 2009 Dec and 2010 Jan. The shaded area indicates the 1σ range of the spectrum gained by forward unfolding, the crosses are from the unfolding after Tikhonov & Arsenin (1979) for comparison. The dark grey area is the spread of the EBL corrected, mean flux values obtained by the four applied EBL models, assuming the redshift of $z=0.444$. The Veritas spectrum after Acciari et al. (2009) is shown for comparison.

TABLE 1
EBL CORRECTED INDICES

model	Γ_{int}
Franceschini et al. (2008)	2.57 ± 0.68
Gilmore et al. (2009)	2.61 ± 0.67
Domínguez et al. (2010)	2.59 ± 0.68
Kneiske & Dole (2010)	2.37 ± 0.70